

# 1 From Canals to the Coast: Dissolved Organic Matter and Trace 2 Metal Composition in Rivers Draining Degraded Tropical 3 Peatlands in Indonesia

4 Laure Gandois<sup>a</sup>, Alison M. Hoyt<sup>b\*</sup>, Stéphane Mounier<sup>c</sup>, Gaël Le Roux<sup>a</sup>, Charles F. Harvey<sup>bd</sup>,  
5 Adrien Claustres<sup>a</sup>, Mohammed Nuriman<sup>e</sup>, Gusti Anshari<sup>c</sup>

6 <sup>a</sup> EcoLab, Université de Toulouse, CNRS, INPT, UPS, Toulouse, France

7 <sup>b</sup>Department of Civil & Environmental Engineering, Massachusetts Institute of Technology, Cambridge, MA  
8 01239, USA

9 <sup>c</sup>PROTEE, Université de Toulon, F-83957, La Garde, France

10 <sup>d</sup> Center for Environmental Sensing and Modeling, Singapore MIT Alliance for Research and Technology,  
11 Singapore

12 <sup>e</sup>Magister of Environmental Science, and Soil Science Department, Universitas Tanjungpura (UNTAN),  
13 Pontianak, West Kalimantan Province, Indonesia

14 \*Present address: Max Planck Institute for Biogeochemistry, 07745 Jena, Germany

15 Corresponding author: ahoyt@bgc-jena.mpg.de  
16

17 **Abstract.** Worldwide, peatlands are important sources of dissolved organic matter (DOM) and trace metals (TM)  
18 to surface waters and these fluxes may increase with peatland degradation. In Southeast Asia, tropical peatlands  
19 are being rapidly deforested and drained. The black rivers draining these peatland areas have high concentrations  
20 of DOM, and the potential to be hotspots for CO<sub>2</sub> release. However, the fate of this fluvial carbon export is  
21 uncertain, and its role as a trace metal carrier has never been investigated. This work aims to address these gaps in  
22 our understanding of tropical peatland DOM and associated elements in the context of degraded tropical peatlands  
23 in Indonesian Borneo. We quantified dissolved organic carbon and trace metal concentrations in the dissolved and  
24 fine colloidal (<0.22µm) and coarse colloidal (0.22 – 2.7 µm) fractions and determined the characteristics ( $\delta^{13}\text{C}$ ,  
25 Absorbance, Fluorescence: excitation-emission matrix and PARAFAC analysis) of the peatland-derived DOM as  
26 it drains from peatland canals, flows along the Ambawang River, a black river, and eventually mixes with the  
27 Kapuas Kecil River (white river) before meeting the ocean near the city of Pontianak in West Kalimantan,  
28 Indonesia. We observe downstream shifts in indicators of in-stream processing. An increase in the  $\delta^{13}\text{C}$  of DOC,  
29 along with an increase in the C1/C2 ratio of PARAFAC fluorophores, and decrease in SUVA (Specific UV  
30 Absorbance) along the continuum suggest the predominance of photo-oxidation. However, very low dissolved  
31 oxygen concentrations also suggest that oxygen is quickly consumed by microbial degradation of DOM in the  
32 shallow layers of water. Black rivers draining degraded peatlands show significantly higher concentrations of Al,  
33 Fe, Pb, As, Ni, and Cd, compared the white river. A strong association is observed between DOM, Fe, As, Cd and  
34 Zn in the dissolved and fine colloid fraction, while Al is associated with Pb and Ni and present in a higher  
35 proportion in the coarse colloidal fraction. We additionally measured the isotopic composition of lead released  
36 from degraded tropical peatlands for the first time and show that Pb originates from anthropogenic atmospheric

37 deposition. Degraded tropical peatlands are important sources of DOM and trace metals to rivers and a secondary  
38 source of atmospherically deposited contaminants.

39 **Keywords:** Tropical peatlands, Dissolved Organic Matter, Absorbance, Fluorescence, PARAFAC, Stable  
40 isotopes, Trace metal, Lead isotopes

## 41 **1. Introduction**

42 Most Southeast Asian tropical peatlands developed as domes beneath ombrotrophic peat swamp forests (Page et  
43 al., 2006; Cobb et al. 2017). They store at least 68.5 Pg C, or 15-19% of the global peat carbon stocks (Dargie et  
44 al., 2017; Lahteenoja et al., 2009; Page et al., 2011). They have experienced widespread degradation as a result of  
45 deforestation, conversion to agriculture and drainage, which all accelerated in the late 2000s. This abrupt change  
46 in land use, and corresponding lowering of the water table, has led to subsidence and a massive release of carbon  
47 from peatlands to the atmosphere due to enhanced aerobic decomposition of organic matter from the drained peat.  
48 Extensive work has focused on quantifying the resulting CO<sub>2</sub> fluxes (Couwenberg et al., 2010; Hoyt et al., 2019;  
49 Jauhiainen et al., 2012; Miettinen et al., 2017) and land surface subsidence (e.g. Hooijer et al., 2012; Carlson et  
50 al., 2015).

51 Drainage canals are dug in forested peatlands for multiple reasons: first, as a mechanism to transport timber out of  
52 the peatland during deforestation, and later to lower the water table, making the land suitable for agriculture. These  
53 peatland drainage canals channel water from the peatlands to surrounding surface waters. The resulting fluvial  
54 export of dissolved organic matter (DOM) has been recognized as an important component of the carbon budget  
55 of tropical peatlands, that could increase with deforestation and peatland exploitation (Gandois et al., 2013; Moore  
56 et al., 2011). Indonesia alone contributes over 10% of the global riverine dissolved organic carbon (DOC) input  
57 into the ocean (Baum et al., 2007), as a result of both high peatland coverage and high precipitation rates. This  
58 proportion is likely to increase with rapid peatland conversion to agriculture, which destabilizes long-term peat C  
59 stocks (Moore et al., 2013).

60 Another implication of DOM transfers from peatlands to surface water is the transport of associated elements,  
61 especially trace metals (TM). Tropical peatlands in Southeast Asia are mainly ombrotrophic systems, which  
62 receive critical nutrients through atmospheric deposition, and serve as a sink for atmospheric pollutants (Weiss et  
63 al., 2002). Northern peatlands have been shown to constitute a source of major and trace elements to surface waters  
64 (Broder and Biester, 2017; Jeremiason et al., 2018; Rothwell et al., 2007). This has important implications: as a  
65 result of colloidal association between peatland-derived organic molecules and Fe, northern peatlands are  
66 responsible for a significant transfer of Fe to the Atlantic Ocean (Krachler et al. 2010, 2012). In the UK, peat  
67 degradation and erosion has led to the dispersion of lead into watersheds, which previously accumulated through  
68 atmospheric deposition over decades (Rothwell et al., 2008). Although drainage of tropical peatlands is occurring  
69 at a rapid rate across Southeast Asia, to our knowledge no data are available on trace metal release in black rivers  
70 draining tropical peatlands.

71 Black rivers draining peatlands (as defined in Alkhatib et al., (2007)) also have the potential to be hotspots of  
72 fluvial carbon degassing (Muller et al., 2015; Wit et al., 2015). By measuring pCO<sub>2</sub> in Indonesian and Malaysian

73 black rivers, Wit et al. (2015) estimated that 53% of DOC entering surface waters was converted to CO<sub>2</sub>, which is  
74 similar to global averages for inland waters. In contrast, black river measurements and incubations by Martin et  
75 al., (2018) found a smaller proportion of DOC was processed in rivers. Rixen et al., (2008) also found a large  
76 proportion of the DOM was resistant to decomposition in a laboratory incubation study. These studies have focused  
77 on CO<sub>2</sub> measurements and incubations to assess the potential for DOM processing.

78 Monitoring both isotopic and optical characteristics of DOM composition in canals and rivers can provide  
79 complementary information on the extent of in-stream processing of fluvial carbon, and potential emission of  
80 greenhouse gases (GHGs) to the atmosphere. Qualitative evaluation of in-stream DOM transformation by UV light  
81 and microbial processes can be performed using isotopic and optical characterization of DOM. The stable isotope  
82 signature of DOM is both an indicator of its origin (Barber et al., 2017; Hood et al., 2005), as well as transformation  
83 processes. Lalonde et al. (2014) assessed photochemical processing of DOM in major rivers worldwide, and found  
84 that it caused an increase in the  $\delta^{13}\text{C}$  of DOM of 0.5 to 2.3‰. Similarly, microbial processing is also expected to  
85 lead to an increase in the  $\delta^{13}\text{C}$  of DOM. Optical properties of DOM are also sensitive indicators of DOM processing  
86 (Hansen et al., 2016; Harun et al., 2015; Spencer et al., 2009). However, in contrast to the  $\delta^{13}\text{C}$  of DOM, which is  
87 similarly enriched by both microbial processing and photo-oxidation, the optical properties of DOM change in  
88 opposite directions in response to microbial processing or photo-oxidation. Microbial processing is generally found  
89 to increase the aromaticity of DOM by selective processing of less aromatic molecules, while photo-oxidation  
90 tends to decrease aromaticity, because of selective photo-oxidation of aromatic moieties (Spencer et al., 2009;  
91 Hansen et al., 2016).

92 In summary, although there has been an increase in efforts to quantify DOC exports from tropical peatlands, our  
93 complementary understanding of the transfer of associated elements and in-stream processing of DOM remains  
94 limited. This work aims to address these gaps in our understanding of the composition and evolution of tropical  
95 peatland DOM and how it could act as a carrier of trace metals to surface waters, in the context of highly degraded  
96 tropical peatlands in Indonesia. We characterize the quality of the peatland-derived DOM and trace metals as they  
97 drain from peatland canals, flow along black rivers, and eventually mix with a white water river before meeting  
98 the ocean. We assess spatial and seasonal changes in the organic matter quality, and document changes in DOM  
99 composition due to transport, mixing, and processing. We also assess black river trace metal release to surface  
100 waters, analyzing trace metal concentrations and the isotopic composition of lead released from degraded tropical  
101 peatlands for the first time.

## 102 **2. Material and methods**

### 103 **2.1 Study area**

104 The study area is located in West Kalimantan, Indonesia, near the city of Pontianak (0.09°N, 109.24°E) on the  
105 island of Borneo (Figure 1). The climate is humid equatorial with 2953±564 mm of rainfall and a mean annual  
106 temperature of 27°C (1985-2017 data). The monthly annual rainfall ranges from 170±126 mm (August) to 349±98  
107 mm (November). The highest rainfalls are measured from October to January. The mean rainfall is 274 ± 123 mm  
108 for January, and 199 ± 106 mm for June. (Figure SI.1). The study focused on the Ambawang River, which flows  
109 into the Landak river, which in turn flows into Kapuas Kecil river. It is a black river draining a watershed

110 (approximately 706 km<sup>2</sup>) entirely covered with peatlands. This river was selected to represent water of  
111 exclusively peatland origin. All peatlands in the sampling area have been drained and converted to agriculture.  
112 Current land use consists of small scale rubber plantation, secondary forest, oil palm plantation, and human  
113 settlements.

## 114 **2.2 Sample collection and treatment**

115 Two sampling campaigns were conducted in June 2013 (drier period) and January 2014 (wetter period). Using a  
116 boat, samples were collected in the center of the river, from the origin of the Ambawang river (BR, black river  
117 sites) to its downstream confluence with the Landak and Kapuas Kecil Kecil (WR, white river sites). White river  
118 samples collected upstream of the confluence with the white river (WRu, white river upstream). Drainage canals  
119 (DC) flowing into the black river were also sampled during the second sampling campaign (Figure 1). In January  
120 2014, a rain collector was installed on the roof of the Pontianak's meteorological station to collect rain samples  
121 for lead isotopic analysis. In situ parameters (pH, conductivity and dissolved oxygen) were measured using a  
122 multiparameter probe (WTW, Germany). Depth profiles of dissolved oxygen in the black river were also measured  
123 with an oxygen microelectrode (MI-730 dip-type micro-oxygen electrode and O2-ADPT adapter; Microelectrodes,  
124 Inc., Bedford, NH, USA). Frequent calibration was performed with a zero oxygen solution and distilled water  
125 equilibrated to ambient oxygen concentrations, where temperature was carefully monitored. To create the zero  
126 oxygen solution, 1 g of sodium sulfite (Na<sub>2</sub>S<sub>2</sub>O<sub>3</sub>) and a few crystals (~1 mg) of cobalt chloride (CoCl<sub>2</sub>) was  
127 dissolved in 1 L of distilled water. For measurements of additional parameters, a larger volume of water was  
128 collected for further analysis. Samples were filtered immediately following collection on the boat using a portable  
129 peristaltic pump (Geotech, USA) and prebaked (5h, 450°C) and pre-weighed GF/F filters (0.7 µm) and stored in  
130 glass bottles for DOC, δ<sup>13</sup>C-DOC and optical properties of DOM analysis, and acidified with HCl for DOC and  
131 δ<sup>13</sup>C-DOC. Samples were filtered with cellulose acetate filters (0.22 µm), acidified with HNO<sub>3</sub> and stored in  
132 polypropylene vials for analysis of major nutrients and trace element. DOC analysis was repeated on the cellulose  
133 acetate samples and DOC concentrations did not differ significantly based on filtration at 0.2 or 0.7 µm. In January  
134 2014, at selected sites (8), samples were first filtered with GF/D filters (2.7µm) to assess to the coarse colloidal  
135 fraction of trace metals and DOC.

## 136 **3. Sample analysis**

137 Non-purgeable organic carbon (NPOC, referred to hereafter as DOC) was analyzed on filtered (GF/F Whatman)  
138 samples after acidification to pH 2 (HCl) with a TOC-V CSH analyzer (Shimadzu, Japan), with a quantification  
139 limit of 1 mg L<sup>-1</sup>. Major cations and anions were analysed using an HPLC (Dionex, USA). The quantification limit  
140 was 0.5 mg L<sup>-1</sup> for chloride, nitrate and sulphates and 0.025 mg L<sup>-1</sup> for ammonium, potassium, magnesium and  
141 calcium. Certified material (ion 915 and ion 96.4 Environment and Climate Change Canada, Canada) was included  
142 in the analytical loop and recovery was >95% of the certified value. For trace element analysis, samples were  
143 acidified with ultrapure HNO<sub>3</sub> prior to ICP-MS (7500 ce, Agilent Technologies) analysis. <sup>115</sup>In was used as an  
144 internal standard, and SLRS-4 (River water certified for trace elements) was used as a reference material on every  
145 run and accuracy (recovery>95%) was checked. Determination limits were < 0.5 µg g<sup>-1</sup> for Fe and Al, <0.05 µg g<sup>-1</sup>  
146 <sup>1</sup> for Ni, Cu and Zn and < 0.005 µg g<sup>-1</sup> for Cd and Pb. Pb isotope ratios (<sup>206</sup>Pb/<sup>207</sup>Pb; <sup>208</sup>Pb/<sup>206</sup>Pb) in water samples

147 were analyzed using a High Resolution ICP-MS (Thermo Element II XR; OMP service ICP-MS, Toulouse,  
148 France). Measurements were corrected for mass bias using individual sample bracketing with certified and  
149 adequately diluted NIST NBS-981 (100 ng L<sup>-1</sup> to 500 ng L<sup>-1</sup>) according to Krachler et al. (2004).

150 The UV absorption spectra of pore water were measured with a spectrophotometer (Secoman UVi-lightXT5) from  
151 190 to 700 nm in a 1 cm quartz cell. The Specific UV Absorbance at 254 nm (SUVA, L mg<sup>-1</sup> m<sup>-1</sup>) was calculated  
152 as follows:  $SUVA = A_{254}/(b \cdot DOC)$  (Weishaar et al., 2003), where  $A_{254}$  is the sample absorbance at 254 nm (non-  
153 dimensional),  $b$  is the optical path length (m) and DOC is in mg L<sup>-1</sup>. The baseline was determined with ultra-pure  
154 water. Potential additional absorbance related to Fe content was following the procedure described by Poulin et  
155 al., (2014). The additional absorbance was small, and represented only  $3.6 \pm 1.4\%$  of the total absorbance across  
156 all samples and was therefore neglected.

157 Emission Excitation Matrices (EEM) were acquired using a Hitachi F4500 fluorescence spectrometer, and  
158 instrument specific correction were applied. Emission spectra were acquired from 250 to 550 nm for excitation  
159 ranging from 250 to 550 nm. The slits were set to 5 nm for both the excitation and emission monochromators. The  
160 scan speed was 2400 nm min<sup>-1</sup> and the integration response was 0.1 s. Fluorescence intensity was corrected from  
161 the excitation beam to ensure stability. The inner filter effect water was taken into account using a dilution  
162 approach as developed by Luciani et al. (2009). The fluorescence index was calculated as defined by McKnight et  
163 al. (2001) and Jaffé et al. (2008), by the ratio of the fluorescence intensity at 470 nm to the fluorescence intensity  
164 at 520 nm for a 370 nm excitation. The shape of the excitation spectra was checked following the recommendation  
165 of Cory et al., (2010). The PARAFAC analysis (PARAllel FACtor analysis (Bro, 1997)) was performed on all  
166 samples using the PROGMEEF program in Matlab (Luciani et al., 2008).

167 The isotopic composition ( $\delta^{13}C$ ) of DOC was determined at the UC Davis Stable Isotope Facility, following the  
168 described procedure (<http://stableisotopefacility.ucdavis.edu/doc.html>). Briefly, a TOC Analyzer (OI Analytical,  
169 College Station, TX) is interfaced to a PDZ Europa 20-20 isotope ratio mass spectrometer (Sercon Ltd., Cheshire,  
170 UK) utilizing a GD-100 Gas Trap Interface (Graden Instruments).

#### 171 **4. Statistical analysis**

172 Statistical analysis was performed using R (R Core Team, 2019) and the R studio software (Version 1.2.1335),  
173 using ggplot (Wickham, 2016), dplyr (Wickham et al., 2019), and dunn.test (Dinno, 2017) packages. Significant  
174 differences ( $p < 0.05$ ) between groups were evaluated using Kruskal Wallis and Dunn's post hoc multiple test.

#### 175 **5. Results**

##### 176 **5.1. Trends in water chemistry from the source of the black river to the ocean**

177 The observed water chemistry of the Ambawang river and drainage canals is typical of black rivers draining  
178 peatlands (Table 1, Figure 2), and does not show significant differences between the two sampling seasons. It is  
179 acidic with a pH of  $3.2 \pm 0.6$  and  $3.5 \pm 0.3$  in the drainage canals (DC) and black river (BR) respectively, has a  
180 low conductivity (DC:  $89.8 \pm 21.4 \mu S cm^{-1}$ , BR:  $85.2 \pm 21.6 \mu S cm^{-1}$ ), is hypoxic (DC:  $2.3 \pm 0.3$ , BR:  $1.9 \pm 0.7 mg$

181 L<sup>-1</sup>), and has low nutrient concentrations (DIN < 0.3 mg L<sup>-1</sup> and P-PO<sub>4</sub> < 0.015 mg L<sup>-1</sup>) but high DOC  
182 concentrations (DC: 35.2 ± 5.9, BR: 35.8 ± 3.5 mg L<sup>-1</sup>). The Cl<sup>-</sup> concentrations are low and homogeneous (DC:  
183 2.6 ± 0.7, BR: 2.4 ± 0.6 mg L<sup>-1</sup>). After the confluence with the white river, the chemistry of the river radically  
184 changes. An abrupt increase in pH is observed (WR: 5.3 ± 0.7). The dissolved oxygen concentration increases to  
185 3.7±1.0 mg L<sup>-1</sup>, while DOC concentrations drop sharply to 9.2 ± 3.2 mg L<sup>-1</sup>. We also observe a slight increase in  
186 NO<sub>3</sub><sup>-</sup> and decrease in PO<sub>4</sub><sup>2-</sup>. Across all samples, the DOC concentrations show a significant negative correlation  
187 with DO concentrations (r<sup>2</sup>=0.63, n=40, p<4.10<sup>9</sup>). In contrast, no increase in Cl<sup>-</sup> concentration is observed until  
188 close to the ocean (3 samples corresponding to ocean water intrusion were excluded from Figure 2).

## 189 **5.2. DOM optical characteristics and stable isotopic signature**

190 No systematic differences are observed for the DOM characteristics between the two sampling campaigns. The  
191 δ<sup>13</sup>C signature of DOC (Figure 3a) is very negative, reaching -30.3±0.4‰ in the drainage canals. It gradually and  
192 continually increases along the continuum from upstream in the black river to the ocean (Figure 3a). As a result,  
193 the δ<sup>13</sup>C of DOC in the drainage canals and the black river, is significantly more depleted than the white river. The  
194 δ<sup>13</sup>C signature of DOC is significantly negatively correlated with DOC concentration (r<sup>2</sup>=0.68, p<10<sup>-4</sup>, n=40), with  
195 the highest DOC values being associated with the lowest δ<sup>13</sup>C-DOC values.

196 The SUVA index (Figure 3b) has high values in the black river (5.3±1.2), with the highest values measured  
197 upstream. A wide range of values is measured in the drainage canals (4.3 ±1.4). The SUVA values of the black  
198 river are significantly higher than those measured in the Kapuas Kecil (4.5±0.3) and its tributaries (4.2 ±0.2). The  
199 fluorescence index has relatively high values for tropical peatlands, where most DOM mostly originates is of  
200 terrestrial origin (Gandois et al., 2014; Zhou et al., 2019). The values varies widely in the drainage canals  
201 (1.60±0.17) and black river (1.55±0.06), but is more uniform in the white river, both upstream (1.55±0.03) and  
202 downstream (1.55±0.05) of the confluence with the black river. Despite the high FI values, these two optical  
203 indices show coherent spatial patterns within the black river and drainage canals (Figure 3b&d). For example,  
204 lower SUVA values are associated with higher FI values, in three drainage canals and in the black river close to  
205 their connection, sampled during the second sampling campaign. Across all samples, a significant correlation is  
206 observed between FI and SUVA values (r<sup>2</sup>=0.37, p<10<sup>-4</sup>, n=41).

207 The EEMS of all water samples have two main peaks (Figure SI.2). The primary peak (λ<sub>ex</sub>=250 nm, λ<sub>em</sub>= 460  
208 nm), is coupled with a less intense peak (λ<sub>ex</sub>=350 nm, λ<sub>em</sub>= 460 nm). The peaks are typical of high molecular  
209 and aromatic molecules, which have been observed in wetlands (Fellman et al., 2009). The PARAFAC analysis  
210 reveals two fluorophores: C1 (λ<sub>ex</sub>=255 nm, λ<sub>em</sub>= 450 nm) and C2 (λ<sub>ex</sub>=285 nm, λ<sub>em</sub>= 485 nm, Figure SI. 3) The  
211 first component constitutes from 60 to 73 % of the total fluorescence of samples. The relative contribution of these  
212 two fluorophores evolves along the sampled continuum, with the lowest values measured upstream in the black  
213 river (Figure 3c). The spatial evolution of the C1/C2 ratios and the δ<sup>13</sup>C-DOC values show consistent trends. A  
214 significant (r<sup>2</sup>=0.43, p< 0.001, n=41) relationship is observed across all the samples between these two indicators.  
215 A stronger relationship (r<sup>2</sup>=0.85, p< 0.001, n=5) is observed when the drainage canals samples alone are  
216 considered.

### 217 **5.3. Trace element concentrations and physical fractionation**

218 Black rivers originating from drained peatlands have a unique composition of inorganic elements. The  
219 concentrations of trace metals (Pb, Ni, Zn, Cd) as well as Al and Fe and are significantly higher in the black river  
220 and drainage canals than the concentrations in the white river (Table 2, Figure 4). For Al, Fe and As, high  
221 concentrations are measured in the black river during the first sampling campaign (drier conditions). In contrast to  
222 other TM, higher Cu concentrations are measured in the white river. A PCA analysis (Figure 5) of TM  
223 concentration and DOM properties reveals specific associations between DOC, Fe and As and to a lesser extend  
224 Zn and Cd, while another group is formed by Al, Pb and Ni. Cu shows no association with DOM but does show  
225 increased concentrations with higher FI. The first axis of PCA (load of DOC, Fe, As) strongly discriminates the  
226 black river and drainage canals samples from the white river.

227 The distributions of DOC and TM are presented in Table 3. Dissolved organic carbon is mostly (>98%) dissolved  
228 or in the form of fine colloids (<0.22  $\mu\text{m}$ ) along the entirety of the studied continuum. Iron and As are mostly  
229 present in dissolved form or as fine colloids in the black river and drainage canals (>96%). However, after transfer  
230 to the white river, half of Fe and a third of As is present in the coarse colloidal form. Zinc and Cd do not show  
231 similar patterns. Aluminium is mostly present in the coarse colloidal phase (>60%) in the black river and drainage  
232 canals and this proportion further increases in the white river (>80%). Lead is mostly present in the dissolved and  
233 fine colloid phase (>75%) in the drainage canals and black river and shifts to coarse colloidal (>60%) forms after  
234 the confluence with the white river. Nickel and Cu are mostly present in the dissolved and fine colloidal phase in  
235 the DC and BR but almost entirely in the coarse colloidal fraction in the white river.

### 236 **5.4. Pb isotopic composition**

237 We observe distinct differences between the lead isotope ratios in the white river and those in the black river and  
238 drainage canals. A decrease in the  $^{206}\text{Pb}/^{207}\text{Pb}$  isotopic ratio is observed with increasing Pb concentrations in the  
239 black river but not the white river (Figure 6a). Furthermore, the biplot of the  $^{206}\text{Pb}/^{207}\text{Pb}$  and the  $^{208}\text{Pb}/^{206}\text{Pb}$   
240 signatures illustrate significant differences between the white water and black river/drainage canal groups (Figure  
241 6b).

## 242 **6. Discussion**

### 243 **6.1. In-stream processing of DOM in black rivers**

244 We observe in-stream processing of DOM, but the total DOM exported from tropical peatlands exceeds the  
245 processing capacity of the rivers which drain them and a large proportion of DOM is transported to the ocean. We  
246 find persistently high DOC concentrations in both drainage canals and black rivers draining degraded peatlands  
247 consistent with the range of previously reported values in Borneo (Cook et al., 2018; Moore et al., 2011) and in  
248 the upper range of black rivers in Sumatra (Rixen et al., 2008; Baum et al., 2007). We also find indicators of in-  
249 stream processing of DOM. The transformation of DOM we observe along the continuum is likely primarily due  
250 to photo-oxidation with a smaller contribution from microbial processing. We observe an increase in the  $\delta^{13}\text{C}$ -  
251 DOC values along the studied continuum (Figure 3a). This shift toward higher  $\delta^{13}\text{C}$ -DOC is correlated with an

252 increase in the C1/C2 ratio of PARAFAC fluorophores (Figure 3c). The two fluorophores are typical of terrestrial  
253 input of DOM (Yamashita et al., 2008), and similar to observed fluorophores in other black rivers in Borneo  
254 (Harun et al., 2015; Zhou et al., 2019). An increase in this C1/C2 ratio reflects a shift toward lower wavelengths  
255 and therefore toward lower aromaticity and lower molecular weight (Austnes et al., 2010; Zhou et al., 2019).  
256 Moreover, a decreasing trend in SUVA values is observed along the continuum (Figure 3b). These observations  
257 indicate that at our site, aromatic features are preferentially processed in-stream, consistent with a dominant effect  
258 of photo-oxidation (Amon and Benner, 1996; Sharpless et al., 2014; Spencer et al., 2009). This has also been  
259 observed in the Congo River where photo-oxidation led to an increase in  $\delta^{13}\text{C}$ -DOC and a decrease in aromatic  
260 features (Spencer et al., 2009).

261 However, photo-oxidation is not the only process responsible for the processing of DOM. The low oxygen levels  
262 in the black river and drainage canals and the significant relationship between DOC and DO concentrations suggest  
263 that nearly all oxygen entering the well-mixed water is quickly consumed by DOM oxidation (Figure 2a&b).  
264 Furthermore, the sharply decreasing oxygen profiles measured in the black river suggest that the transformation  
265 of DOM is restricted to the shallow surface layers of these waters (Figure SI.3). Additionally, localized increases  
266 in fluorescence index, coupled with decreases in SUVA (reflecting a higher proportion of microbial derived DOM,  
267 Figure 3d) suggest that microbial processing occurs in some locations in drainage canals. Both photo-oxidation  
268 and microbial processing have been quantified in laboratory experiments for DOM originating from tropical  
269 peatlands. Martin et al. (2018) found that up to 25 % of riverine DOC from a black river in Sarawak, Malaysia,  
270 was lost within 5 days of exposure to natural sunlight. Microbial long-term incubation studies by (Rixen et al.,  
271 2008), showed that 27% of DOC was degraded after two weeks. In black rivers, it is likely that in-stream microbial  
272 processing of DOM is limited by the low oxygen concentrations, low pH, and low nutrient levels (especially  
273 inorganic nitrogen), (Wickland et al., 2012), rather than intrinsic refractory characteristics. Although the precise  
274 extent of in-stream processing cannot be quantified here, our results are consistent with in stream transformation  
275 of DOM by photo-oxidation as well as some contribution of microbial degradation in the shallow surface layers.  
276 In the future, quantitative assessment of outgassing in tropical peatland drainage canals would improve the  
277 evaluation of carbon release following peatland drainage. Overall, more work is needed to understand the extent  
278 of upstream processing of peatland DOM.

## 279 **6.2. Role of DOM, Al and Fe in trace metal dynamics in peat draining waters**

280 This study provides the first record of trace metals in black rivers originating from degraded tropical peatlands.  
281 We observe strong enrichment of Al and Fe, as well as Pb, As, Ni and Cd in peat-draining waters. The measured  
282 concentrations are comparable to those measured by Kurasaki et al. (2000) in Borneo rivers for Pb, Zn, Cu and  
283 Cd, but significantly higher (5 to 10 times) for Fe. The concentration levels, however, remain low compared to  
284 highly impacted regions of Indonesia (Arifin et al., 2012). The elevated concentrations of Al and Fe in water  
285 draining tropical peatlands is consistent with existing observations of elevated Fe concentrations from black rivers  
286 in the tropics (Zhang et al., 2019) and northern peatlands. This enrichment is likely due to the weathering of mineral  
287 material under the peat during peat accumulation processes (Tipping et al., 2002; Pokrovsky et al., 2005). As a  
288 consequence, in water draining peatlands, strong organo-mineral associations between DOM and Fe (Krachler et  
289 al. 2010, 2012; Broder and Biester 2015), as well as DOM and Al (Helmer et al., 1990) have been observed. These



290 colloidal associations between DOM and Al and Fe in the form of hydroxides strongly control TM transfer and  
291 speciation in peat draining waters (Tipping et al., 2002). In the present study, specific associations of trace metals  
292 with Al and Fe are observed, including strong links between Al and Pb and Ni. However, the lack of a direct  
293 relationship between Pb and DOM contrasts with reported observations in the literature (Graham et al., 2006;  
294 Jeremiason et al., 2018; Pokrovsky et al., 2016). Despite this, we do observe strong links between Fe, As, Zn, Cd  
295 and DOM, which have been previously reported in water draining peatlands ( Broder and Biester, 2015; Neubauer  
296 et al., 2013; Pokrovsky et al., 2016). The coupled dynamics of Fe and As might be related to similar mobilization  
297 processes within the peat column, with the sorption of As to Fe(III)-(oxyhydr)oxides (ThomasArrigo et al., 2014)  
298 in anoxic peat water. Widespread drainage of tropical peatlands and the corresponding release of anoxic water to  
299 surface water networks could induce a coupled increase in DOM and Fe concentrations, similar to that which has  
300 occurred in Sweden (Kritzberg and Ekström, 2011).

### 301 **6.3. Peatlands as secondary sources of atmospheric pollutants**

302 The isotopic composition of Pb in peat draining water strongly suggests it is of anthropogenic origin. The isotopic  
303 signatures measured in river samples are a combination of the signature of undisturbed soils of Borneo (Valentine  
304 et al., 2008), and a mix of both present and past anthropogenic inputs. Older anthropogenic inputs are reflected by  
305 the signature of atmospheric deposition from Java aerosols (Bollhöfer and Rosman, 2000), while the signature of  
306 recent regional anthropogenic inputs was characterized by rain samples collected in Pontianak as part of this study  
307 (Figure 6b). In the black river and drainage canals, the isotopic ratio is close to that of aerosols and recently sampled  
308 rainwater and is dominated by anthropogenic inputs, whereas the isotopic ratio in the white river is closer to the  
309 natural signal (Figure 6). This isotopic difference is consistent with the difference between the watersheds drained  
310 by these two rivers: tropical peatlands are ombrotrophic systems, and the trace metal content in peat soil is derived  
311 from the atmosphere (Weiss et al., 2002), whereas the Kapus Kecil is recharged from a larger watershed and  
312 reflects contribution of mineral soils. Tropical peatlands can serve as secondary sources of atmospheric pollutants  
313 to the environment. With peatland drainage, black rivers release the accumulated atmospheric deposition over  
314 hundreds of years on much shorter timescales. For example, the isotopic signature observed in the black river  
315 reflects anthropogenic sources deposited at different times, including older deposition such as the lead measured  
316 in the Java aerosols (Bollhöfer and Rosman, 2000), and more recent deposition following the widespread  
317 introduction of unleaded fuel (characterized by samples collected from rainwater during the January 2014 sampling  
318 period in this study). This release of lead by degraded tropical peatlands has the potential to impact records from  
319 environmental archives, for example the corals of the Singapore Strait (Chen et al., 2015). Although this is the  
320 first measurement of the aquatic release of trace metals from tropical peatlands, the role of tropical peatlands as a  
321 secondary source of contaminants has also been highlighted by the trace metal content analysis of dust emitted to  
322 the atmosphere by peat fires (Betha et al., 2013).

### 323 **6.4. From degraded tropical peatlands to the ocean**

324 Sharp changes in physico-chemical conditions are observed after the mixing of the black and the white river,  
325 including sharp increases in DO concentrations and pH values. This strongly controls the transport of DOM and  
326 TM drained from degraded tropical peatlands. After the confluence with the white river, DOC concentrations  
327 decrease abruptly. This decrease primarily results from the dilution of the black river signal. However, the sudden

328 elevation of pH and DO after the confluence might create favorable conditions for microbial processing of DOC,  
329 making the mixing zone a likely hotspot of GHG emissions (Palmer et al., 2016).. This would also be consistent  
330 with the decrease in the SUVA index observed after the confluence. Despite processing of DOM along the  
331 continuum, a significant proportion of DOM originating from degraded peatlands actually reaches ocean. We  
332 observe high DOC concentrations at all sampling locations, with concentrations remaining high even close to the  
333 ocean (Figure 2a). Additionally, the results of our physical fractionation show that even close to the estuary, DOC  
334 remains in the dissolved and fine colloid form ( $<0.22 \mu\text{m}$ ), and that flocculation processes might be limited. Then,  
335 the important proportion of coastal peatlands in Indonesia and Malaysia results in the relatively high fluvial organic  
336 carbon export reported in to South China Sea (Huang et al., 2017).The decrease in trace metal concentrations after  
337 the confluence might be influenced by shifts in physical fractionation and an increased proportion of colloidal  
338 form. This is especially true for Al and Pb. Some flocculation at the estuary might limit their transfer to the ocean.  
339 For Fe and As, a higher proportion remains in the form of fine colloids after mixing with the whiter river, and is  
340 still associated with DOC. Similar conservative behavior of LMW organic molecules associated with Fe was  
341 observed at the outlet of northern peatlands (Krachler et al., 2012), and in Arctic rivers (Pokrovsky et al., 2014).  
342 This highlights that dissolved organic molecules derived from tropical peatlands can also act as carriers of trace  
343 metals to the ocean.

## 344 **7. Conclusions**

345 This study characterizes the composition and concentration of DOM and TM in the canals and rivers draining the  
346 degraded tropical peatlands of Indonesian Borneo. It highlights in-stream processing of DOM in drainage canals  
347 and rivers draining degraded peatlands. Both stable isotopic and optical properties of DOM are consistent with  
348 photo-oxidation along the continuum from the black river to the ocean. In the black river and drainage canals, rates  
349 of microbial processing are likely limited by the low dissolved oxygen concentrations, and limited to shallow  
350 depths. Along the continuum, DOM is found at relatively high concentrations in the dissolved and fine colloidal  
351 phases, suggesting a substantial fraction of DOM derived from degraded peatlands reaches the ocean. Additionally,  
352 we provide the first assessment of trace metal concentrations in rivers draining degraded tropical peatlands. Rivers  
353 draining these peatlands are enriched in some trace metals (Pb, Ni, Zn, Cd) as well as Al and Fe. Using the isotopic  
354 signature of Pb, we show that degraded tropical peatlands are secondary sources of atmospherically deposited  
355 contaminants to surface waters. Trace metal dynamics after transfer to the white river show clear trends: while Pb  
356 and Ni are associated with Al; As, Zn and Cd are associated with Fe and DOM. Lead and Al are present in coarse  
357 colloidal form and may be transferred to sediments after flocculation. In contrast, DOM, Fe and As are found  
358 predominantly in fine colloidal form even after the confluence with the white river, and as a result may be  
359 transferred to the ocean. The role of degraded tropical peatlands as a source of DOM, as well as Fe and As to the  
360 ocean requires further investigation.

## 361 **Author contribution**

362 LG, AMH, GH and CFH designed the study. LG, AMH, MN and GH conducted field campaigns. SM and LG  
363 conducted fluorescence analysis. GLR and AC conducted lead isotope analysis. LG and AMH wrote the  
364 manuscript, with inputs from all co-authors.

365 **Competing interests**

366 The authors declare no competing interests.

367 **Data availability**

368 The data are available at <https://doi.org/10.5194/bg-2019-253>.

369 **Acknowledgements**

370 This research was supported by the National Research Foundation Singapore through the Singapore-MIT Alliance  
371 for Research and Technology's Center for Environmental Sensing and Modeling interdisciplinary research  
372 program and Grant No. NRF2016-ITCOO1-021, by the USA National Science Foundation under Grant No.  
373 1923478 to C.F.H, and by the PEER project "Assessing Degradation of Tropical Peat Domes and Dissolved  
374 Organic Carbon (DOC) Export from the Belait, Mempawah and Lower Kapuas Kecil Rivers in Borneo" lead by  
375 G. A.. We thank F. Julien, V. Payre-Suc and D. Lambrigot for DOC and major elements analysis (PAPC platform,  
376 EcoLab laboratory), and F. Candaudap for lead isotope analysis (ICP-MS platform, GET laboratory). We also  
377 thank Patrick Martin and one anonymous reviewer for their constructive comments that improved the manuscript.

378 **References**

- 379 Alkhatib, M., Jennerjahn, T. C. and Samiaji, J.: Biogeochemistry of the Dumai River estuary, Sumatra, Indonesia,  
380 a tropical black-water river, *Limnol. Oceanogr.*, 52(6), 2410–2417, doi:10.4319/lo.2007.52.6.2410, 2007.
- 381 Amon, R. M. W. and Benner, R.: Photochemical and microbial consumption of dissolved organic carbon and  
382 dissolved oxygen in the Amazon River system, *Geochim. Cosmochim. Acta*, 60(10), 1783–1792,  
383 doi:10.1016/0016-7037(96)00055-5, 1996.
- 384 Arifin, Z., Puspitasari, R. and Miyazaki, N.: Heavy metal contamination in Indonesian coastal marine ecosystems:  
385 A historical perspective, *Coast. Mar. Sci.*, 35(1), 227–233, 2012.
- 386 Austnes, K., Evans, C. D., Eliot-Laize, C., Naden, P. S. and Old, G. H.: Effects of storm events on mobilisation  
387 and in-stream processing of dissolved organic matter (DOM) in a Welsh peatland catchment, *Biogeochemistry*,  
388 99(1), 157–173, doi:10.1007/s10533-009-9399-4, 2010.
- 389 Barber, A., Sirois, M., Chaillou, G. and Gélinas, Y.: Stable isotope analysis of dissolved organic carbon in  
390 Canada's eastern coastal waters, *Limnol. Oceanogr.*, 62(S1), S71–S84, doi:10.1002/lno.10666, 2017.
- 391 Baum, A., Rixen, T. and Samiaji, J.: Relevance of peat draining rivers in central Sumatra for the riverine input of  
392 dissolved organic carbon into the ocean, *Estuar. Coast. Shelf Sci.*, 73(3–4), 563–570,  
393 doi:10.1016/j.ecss.2007.02.012, 2007.
- 394 Betha, R., Pradani, M., Lestari, P., Joshi, U. M., Reid, J. S. and Balasubramanian, R.: Chemical speciation of trace  
395 metals emitted from Indonesian peat fires for health risk assessment, *Atmospheric Res.*, 122(Supplement C), 571–  
396 578, doi:10.1016/j.atmosres.2012.05.024, 2013.
- 397 Bollhöfer, A. and Rosman, K. J. R.: Isotopic source signatures for atmospheric lead: the Southern Hemisphere,  
398 *Geochim. Cosmochim. Acta*, 64(19), 3251–3262, doi:10.1016/S0016-7037(00)00436-1, 2000.
- 399 Bro, R.: PARAFAC. Tutorial and applications - ScienceDirect, *Chemom. Intell. Lab. Syst.*, 149–171, 1997.
- 400 Broder, T. and Biester, H.: Hydrologic controls on DOC, As and Pb export from a polluted peatland – the  
401 importance of heavy rain events, antecedent moisture conditions and hydrological connectivity, *Biogeosciences*,  
402 12(15), 4651–4664, doi:<https://doi.org/10.5194/bg-12-4651-2015>, 2015.

403 Broder, T. and Biester, H.: Linking major and trace element concentrations in a headwater stream to DOC release  
404 and hydrologic conditions in a bog and peaty riparian zone, *Appl. Geochem.*, 87, 188–201,  
405 doi:10.1016/j.apgeochem.2017.11.003, 2017.

406 Carlson, K. M., Goodman, L. K. and May-Tobin, C. C.: Modeling relationships between water table depth and  
407 peat soil carbon loss in Southeast Asian plantations, *Environ. Res. Lett.*, 10(7), 074006, doi:10.1088/1748-  
408 9326/10/7/074006, 2015.

409 Chen, M., Lee, J.-M., Nurhati, I. S., Switzer, A. D. and Boyle, E. A.: Isotopic record of lead in Singapore Straits  
410 during the last 50 years: Spatial and temporal variations, *Mar. Chem.*, 168, 49–59,  
411 doi:10.1016/j.marchem.2014.10.007, 2015.

412 Cobb, A. R., Hoyt, A. M., Gandois, L., Eri, J., Dommain, R., Salim, K. A., Kai, F. M., Su'ut, N. S. H. and Harvey,  
413 C. F.: How temporal patterns in rainfall determine the geomorphology and carbon fluxes of tropical peatlands,  
414 *Proc. Natl. Acad. Sci.*, 114(26), E5187–E5196, doi:10.1073/pnas.1701090114, 2017.

415 Cook, S., Whelan, M. J., Evans, C. D., Gauci, V., Peacock, M., Garnett, M. H., Kho, L. K., Teh, Y. A. and Page,  
416 S. E.: Fluvial organic carbon fluxes from oil palm plantations on tropical peatland, *Biogeosciences*, 15(24), 7435–  
417 7450, doi:https://doi.org/10.5194/bg-15-7435-2018, 2018.

418 Cory, R. M., Miller, M. P., McKnight, D. M., Guerard, J. J. and Miller, P. L.: Effect of instrument-specific response  
419 on the analysis of fulvic acid fluorescence spectra, *Limnol. Oceanogr. Methods*, 8(2), 67–78,  
420 doi:10.4319/lom.2010.8.67, 2010.

421 Couwenberg, J., Dommain, R. and Joosten, H.: Greenhouse gas fluxes from tropical peatlands in south-east Asia,  
422 *Glob. Change Biol.*, 16(6), 1715–1732, doi:10.1111/j.1365-2486.2009.02016.x, 2010.

423 Dargie, G. C., Lewis, S. L., Lawson, I. T., Mitchard, E. T. A., Page, S. E., Bocko, Y. E. and Ifo, S. A.: Age, extent  
424 and carbon storage of the central Congo Basin peatland complex, *Nature*, 542(7639), 86–90,  
425 doi:10.1038/nature21048, 2017.

426 Dinno, A.: dunn.test: Dunn's Test of Multiple Comparisons Using Rank Sums. R package version 1.3.5.  
427 <https://CRAN.R-project.org/package=dunn.test>, 2017.

428 Fellman, J. B., Miller, M. P., Cory, R. M., D'Amore, D. V. and White, D.: Characterizing Dissolved Organic  
429 Matter Using PARAFAC Modeling of Fluorescence Spectroscopy: A Comparison of Two Models, *Environ. Sci.*  
430 *Technol.*, 43(16), 6228–6234, doi:10.1021/es900143g, 2009.

431 Gandois, L., Cobb, A. R., Hei, I. C., Lim, L. B. L., Salim, K. A. and Harvey, C. F.: Impact of deforestation on  
432 solid and dissolved organic matter characteristics of tropical peat forests: implications for carbon release,  
433 *Biogeochemistry*, 114(1), 183–199, doi:10.1007/s10533-012-9799-8, 2013.

434 Gandois, L., Teisserenc, R., Cobb, A. R., Chieng, H. I., Lim, L. B. L., Kamariah, A. S., Hoyt, A. and Harvey, C.  
435 F.: Origin, composition, and transformation of dissolved organic matter in tropical peatlands, *Geochim.*  
436 *Cosmochim. Acta*, 137, 35–47, doi:10.1016/j.gca.2014.03.012, 2014.

437 Graham, M. C., Vinogradoff, S. I., Chipchase, A. J., Dunn, S. M., Bacon, J. R. and Farmer, J. G.: Using Size  
438 Fractionation and Pb Isotopes to Study Pb Transport in the Waters of an Organic-Rich Upland Catchment, *Environ.*  
439 *Sci. Technol.*, 40(4), 1250–1256, doi:10.1021/es0517670, 2006.

440 Hansen, A. M., Kraus, T. E. C., Pellerin, B. A., Fleck, J. A., Downing, B. D. and Bergamaschi, B. A.: Optical  
441 properties of dissolved organic matter (DOM): Effects of biological and photolytic degradation, *Limnol.*  
442 *Oceanogr.*, 61(3), 1015–1032, doi:10.1002/lno.10270, 2016.

443 Harun, S., Baker, A., Bradley, C., Pinay, G., Boomer, I. and Liz Hamilton, R.: Characterisation of dissolved  
444 organic matter in the Lower Kinabatangan River, Sabah, Malaysia, *Hydrol. Res.*, 46(3), 411–428,  
445 doi:10.2166/nh.2014.196, 2015.

446 Helmer, E. H., Urban, N. R. and Eisenreich, S. J.: Aluminum geochemistry in peatland waters, *Biogeochemistry*,  
447 9(3), doi:10.1007/BF00000601, 1990.

- 448 Hood, E., Williams, M. W. and McKnight, D. M.: Sources of dissolved organic matter (DOM) in a Rocky  
449 Mountain stream using chemical fractionation and stable isotopes, *Biogeochemistry*, 74(2), 231–255,  
450 doi:10.1007/s10533-004-4322-5, 2005.
- 451 Hooijer, A., Page, S., Jauhiainen, J., Lee, W. A., Lu, X. X., Idris, A. and Anshari, G.: Subsidence and carbon loss  
452 in drained tropical peatlands, *Biogeosciences*, 9(3), 1053–1071, doi:10.5194/bg-9-1053-2012, 2012.
- 453 Hoyt, A. M., Gandois, L., Eri, J., Kai, F. M., Harvey, C. F. and Cobb, A. R.: CO<sub>2</sub> emissions from an undrained  
454 tropical peatland: Interacting influences of temperature, shading and water table depth, *Glob. Change Biol.*, 25(9),  
455 2885–2899, doi:10.1111/gcb.14702, 2019.
- 456 Huang, T. H., Chen, C. T. A., Tseng, H. C., Lou, J. Y., Wang, S. L., Yang, L., Kandasamy, S., Gao, X., Wang, J.  
457 T., Aldrian, E., Jacinto, G. S., Anshari, G. Z., Sompongchaiyakul, P. and Wang, B. J.: Riverine carbon fluxes to  
458 the South China Sea, *J. Geophys. Res. Biogeosciences*, 122(5), 1239–1259, doi:10.1002/2016JG003701, 2017.
- 459 Jaffé, R., McKnight, D., Maie, N., Cory, R., McDowell, W. H. and Campbell, J. L.: Spatial and temporal variations  
460 in DOM composition in ecosystems: The importance of long-term monitoring of optical properties, *J. Geophys.*  
461 *Res. Biogeosciences*, 113(G4), doi:10.1029/2008JG000683, 2008.
- 462 Jauhiainen, J., Hooijer, A. and Page, S. E.: Carbon Dioxide emissions from an Acacia plantation on peatland in  
463 Sumatra, Indonesia, , doi:https://doi.org/10.5194/bg-9-617-2012, 2012.
- 464 Jeremiason, J. D., Baumann, E. I., Sebestyen, S. D., Agather, A. M., Seelen, E. A., Carlson-Stehlin, B. J., Funke,  
465 M. M. and Cotner, J. B.: Contemporary Mobilization of Legacy Pb Stores by DOM in a Boreal Peatland, *Environ.*  
466 *Sci. Technol.*, 52(6), 3375–3383, doi:10.1021/acs.est.7b06577, 2018.
- 467 Krachler, M., Roux, G. L., Kober, B. and Shotyk, W.: Optimising accuracy and precision of lead isotope  
468 measurement ( 206 Pb, 207 Pb, 208 Pb) in acid digests of peat with ICP-SMS using individual mass discrimination  
469 correction, *J. Anal. At. Spectrom.*, 19(3), 354–361, doi:10.1039/B314956K, 2004.
- 470 Krachler, R., Krachler, R. F., von der Kammer, F., Süphandag, A., Jirsa, F., Ayromlou, S., Hofmann, T. and  
471 Keppler, B. K.: Relevance of peat-draining rivers for the riverine input of dissolved iron into the ocean, *Sci. Total*  
472 *Environ.*, 408(11), 2402–2408, doi:10.1016/j.scitotenv.2010.02.018, 2010.
- 473 Krachler, R., von der Kammer, F., Jirsa, F., Süphandag, A., Krachler, R. F., Plessl, C., Vogt, M., Keppler, B. K.  
474 and Hofmann, T.: Nanoscale lignin particles as sources of dissolved iron to the ocean: NANOSCALE LIGNIN  
475 PARTICLES, *Glob. Biogeochem. Cycles*, 26(3), n/a-n/a, doi:10.1029/2012GB004294, 2012.
- 476 Kritzberg, E. S. and Ekström, S. M.: Increasing iron concentrations in surface waters – a factor behind  
477 brownification?, *Biogeosciences Discuss.*, 8(6), 12285–12316, doi:10.5194/bgd-8-12285-2011, 2011.
- 478 Kurasaki, M., Hartoto, D. I., Saito, T., Suzuki-Kurasaki, M. and Iwakuma, T.: Metals in Water in the Central  
479 Kalimantan, Indonesia, *Bull. Environ. Contam. Toxicol.*, 65(5), 591–597, doi:10.1007/s0012800164, 2000.
- 480 Lähteenoja, O., Ruokolainen, K., Schulman, L. and Oinonen, M.: Amazonian peatlands: an ignored C sink and  
481 potential source, *Glob. Change Biol.*, 15(9), 2311–2320, doi:10.1111/j.1365-2486.2009.01920.x, 2009.
- 482 Lalonde, K., Vähätalo, A. and Gélinas, Y.: Revisiting the disappearance of terrestrial dissolved organic matter in  
483 the ocean: a  $\delta^{13}\text{C}$  study, *Biogeosciences*, 11(13) [online] Available from:  
484 <https://jyx.jyu.fi/handle/123456789/44281> (Accessed 16 June 2019), 2014.
- 485 Luciani, X., Mounier, S., Paraquetti, H. H. M., Redon, R., Lucas, Y., Bois, A., Lacerda, L. D., Raynaud, M. and  
486 Ripert, M.: Tracing of dissolved organic matter from the SEPETIBA Bay (Brazil) by PARAFAC analysis of total  
487 luminescence matrices, *Mar. Environ. Res.*, 65(2), 148–157, doi:10.1016/j.marenvres.2007.09.004, 2008.
- 488 Luciani, X., Mounier, S., Redon, R. and Bois, A.: A simple correction method of inner filter effects affecting  
489 FEEM and its application to the PARAFAC decomposition, *Chemom. Intell. Lab. Syst.*, 96(2), 227–238,  
490 doi:10.1016/j.chemolab.2009.02.008, 2009.

- 491 Martin, P., Cherukuru, N., Tan, A. S. Y., Sanwlani, N., Mujahid, A. and Müller, M.: Distribution and cycling of  
492 terrigenous dissolved organic carbon in peatland-draining rivers and coastal waters of Sarawak, Borneo, ,  
493 doi:<http://dx.doi.org/10.5194/bg-15-6847-2018>, 2018.
- 494 McKnight, D. M., Boyer, E. W., Westerhoff, P. K., Doran, P. T., Kulbe, T. and Andersen, D. T.:  
495 Spectrofluorometric characterization of dissolved organic matter for indication of precursor organic material and  
496 aromaticity, *Limnol. Oceanogr.*, 46(1), 38–48, doi:10.4319/lo.2001.46.1.0038, 2001.
- 497 Miettinen, J., Hooijer, A., Vernimmen, R., Liew, S. C. and Page, S. E.: From carbon sink to carbon source:  
498 extensive peat oxidation in insular Southeast Asia since 1990, *Environ. Res. Lett.*, 12(2), 024014,  
499 doi:10.1088/1748-9326/aa5b6f, 2017.
- 500 Moore, S., Gauci, V., Evans, C. D. and Page, S. E.: Fluvial organic carbon losses from a Bornean blackwater river,  
501 *Biogeosciences*, 8, 901–909, 2011.
- 502 Moore, S., Evans, C. D., Page, S. E., Garnett, M. H., Jones, T. G., Freeman, C., Hooijer, A., Wiltshire, A. J., Limin,  
503 S. H. and Gauci, V.: Deep instability of deforested tropical peatlands revealed by fluvial organic carbon fluxes,  
504 *Nature*, 493(7434), 660–663, doi:10.1038/nature11818, 2013.
- 505 Müller, D., Warneke, T., Rixen, T., Müller, M., Jamahari, S., Denis, N., Mujahid, A. and Notholt, J.: Lateral carbon  
506 fluxes and CO<sub>2</sub> outgassing from a tropical peat-draining river, *Biogeosciences Discuss.*,  
507 12(13), 10389–10424, doi:10.5194/bgd-12-10389-2015, 2015.
- 508 Neubauer, E., von der Kammer, F., Knorr, K.-H., Peiffer, S., Reichert, M. and Hofmann, T.: Colloid-associated  
509 export of arsenic in stream water during stormflow events, *Chem. Geol.*, 352, 81–91,  
510 doi:10.1016/j.chemgeo.2013.05.017, 2013.
- 511 Page, S. E., Rieley, J. O. and Wüst, R.: Chapter 7 Lowland tropical peatlands of Southeast Asia, in *Developments*  
512 *in Earth Surface Processes*, vol. 9, edited by I. P. Martini, A. Martínez Cortizas, and W. Chesworth, pp. 145–172,  
513 Elsevier., 2006.
- 514 Page, S. E., Rieley, J. O. and Banks, C. J.: Global and regional importance of the tropical peatland carbon pool,  
515 *Glob. Change Biol.*, 17(2), 798–818, doi:10.1111/j.1365-2486.2010.02279.x, 2011.
- 516 Palmer, S. M., Evans, C. D., Chapman, P. J., Burden, A., Jones, T. G., Allott, T. E. H., Evans, M. G., Moody, C.  
517 S., Worrall, F. and Holden, J.: Sporadic hotspots for physico-chemical retention of aquatic organic carbon: from  
518 peatland headwater source to sea, *Aquat. Sci.*, 78(3), 491–504, doi:10.1007/s00027-015-0448-x, 2016.
- 519 Pokrovsky, O. S., Dupré, B. and Schott, J.: Fe–Al–organic Colloids Control of Trace Elements in Peat Soil  
520 Solutions: Results of Ultrafiltration and Dialysis, *Aquat. Geochem.*, 11(3), 241–278, doi:10.1007/s10498-004-  
521 4765-2, 2005.
- 522 Pokrovsky, O. S., Shirokova, L. S., Viers, J., Gordeev, V. V., Shevchenko, V. P., Chupakov, A. V., Vorobieva, T.  
523 Y., Candaudap, F., Causserand, C., Lanzasova, A. and Zouiten, C.: Fate of colloids during estuarine mixing in the  
524 Arctic, *Ocean Sci.*, 10(1), 107–125, doi:10.5194/os-10-107-2014, 2014.
- 525 Pokrovsky, O. S., Manasypov, R. M., Loiko, S. V. and Shirokova, L. S.: Organic and organo-mineral colloids in  
526 discontinuous permafrost zone, *Geochim. Cosmochim. Acta*, 188, 1–20, doi:10.1016/j.gca.2016.05.035, 2016.
- 527 Poulin, B. A., Ryan, J. N. and Aiken, G. R.: Effects of Iron on Optical Properties of Dissolved Organic Matter,  
528 *Environ. Sci. Technol.*, 48(17), 10098–10106, doi:10.1021/es502670r, 2014.
- 529 R Core Team: A language and environment for statistical computing, R Foundation for Statistical Computing,  
530 Vienna, Austria (<http://R-project.org/>), 2019.
- 531 Rixen, T., Baum, A., Pohlmann, T., Balzer, W., Samiaji, J. and Jose, C.: The Siak, a tropical black water river in  
532 central Sumatra on the verge of anoxia, *Biogeochemistry*, 90(2), 129–140, doi:10.1007/s10533-008-9239-y, 2008.

- 533 Rothwell, J. J., Evans, M. G., Daniels, S. M. and Allott, T. E. H.: Baseflow and stormflow metal concentrations in  
534 streams draining contaminated peat moorlands in the Peak District National Park (UK), *J. Hydrol.*, 341(1), 90–  
535 104, doi:10.1016/j.jhydrol.2007.05.004, 2007.
- 536 Rothwell, J. J., Evans, M. G., Daniels, S. M. and Allott, T. E. H.: Peat soils as a source of lead contamination to  
537 upland fluvial systems, *Environ. Pollut.*, 153(3), 582–589, doi:10.1016/j.envpol.2007.09.009, 2008.
- 538 Sharpless, C. M., Aeschbacher, M., Page, S. E., Wenk, J., Sander, M. and McNeill, K.: Photooxidation-Induced  
539 Changes in Optical, Electrochemical, and Photochemical Properties of Humic Substances, *Environ. Sci. Technol.*,  
540 48(5), 2688–2696, doi:10.1021/es403925g, 2014.
- 541 Spencer, R. G. M., Stubbins, A., Hernes, P. J., Baker, A., Mopper, K., Aufdenkampe, A. K., Dyda, R. Y., Mwamba,  
542 V. L., Mangangu, A. M., Wabakanghanzi, J. N. and Six, J.: Photochemical degradation of dissolved organic matter  
543 and dissolved lignin phenols from the Congo River, *J. Geophys. Res. Biogeosciences*, 114(G3),  
544 doi:10.1029/2009JG000968, 2009.
- 545 ThomasArrigo, L. K., Mikutta, C., Byrne, J., Barmettler, K., Kappler, A. and Kretzschmar, R.: Iron and Arsenic  
546 Speciation and Distribution in Organic Flocs from Streambeds of an Arsenic-Enriched Peatland, *Environ. Sci.*  
547 *Technol.*, 48(22), 13218–13228, doi:10.1021/es503550g, 2014.
- 548 Tipping, E., Rey-Castro, C., Bryan, S. E. and Hamilton-Taylor, J.: Al(III) and Fe(III) binding by humic substances  
549 in freshwaters, and implications for trace metal speciation, *Geochim. Cosmochim. Acta*, 66(18), 3211–3224,  
550 doi:10.1016/S0016-7037(02)00930-4, 2002.
- 551 Valentine, B., Kamenov, G. D. and Krigbaum, J.: Reconstructing Neolithic groups in Sarawak, Malaysia through  
552 lead and strontium isotope analysis, *J. Archaeol. Sci.*, 35(6), 1463–1473, doi:10.1016/j.jas.2007.10.016, 2008.
- 553 Weishaar, J. L., Aiken, G. R., Bergamaschi, B. A., Fram, M. S., Fujii, R. and Mopper, K.: Evaluation of Specific  
554 Ultraviolet Absorbance as an Indicator of the Chemical Composition and Reactivity of Dissolved Organic Carbon,  
555 *Environ. Sci. Technol.*, 37(20), 4702–4708, doi:10.1021/es030360x, 2003.
- 556 Weiss, D., Shotyk, W., Rieley, J., Page, S., Gloor, M., Reese, S. and Martinez-Cortizas, A.: The geochemistry of  
557 major and selected trace elements in a forested peat bog, Kalimantan, SE Asia, and its implications for past  
558 atmospheric dust deposition, *Geochim. Cosmochim. Acta*, 66(13), 2307–2323, doi:10.1016/S0016-  
559 7037(02)00834-7, 2002.
- 560 Wickham, H.: *ggplot2: Elegant Graphics for Data Analysis.*, 2016.
- 561 Wickham, H., François, R., Henry, L. and Müller, K.: *dplyr: A Grammar of Data Manipulation.* R package version  
562 0.8.0.1. <https://CRAN.R-project.org/package=dplyr>, 2019.
- 563 Wickland, K. P., Aiken, G. R., Butler, K., Dornblaser, M. M., Spencer, R. G. M. and Striegl, R. G.:  
564 Biodegradability of dissolved organic carbon in the Yukon River and its tributaries: Seasonality and importance  
565 of inorganic nitrogen, *Glob. Biogeochem. Cycles*, doi:10.1029/2012GB004342@10.1002/(ISSN)1944-  
566 9224.AQUNETWRK1, 2012.
- 567 Wit, F., Müller, D., Baum, A., Warneke, T., Pranowo, W. S., Müller, M. and Rixen, T.: The impact of disturbed  
568 peatlands on river outgassing in Southeast Asia, *Nat. Commun.*, 6, 10155, doi:10.1038/ncomms10155, 2015.
- 569 Yamashita, Y., Jaffé, R., Maie, N. and Tanoue, E.: Assessing the dynamics of dissolved organic matter (DOM) in  
570 coastal environments by excitation emission matrix fluorescence and parallel factor analysis (EEM-PARAFAC),  
571 *Limnol. Oceanogr.*, 53(5), 1900–1908, doi:10.4319/lo.2008.53.5.1900, 2008.
- 572 Zhang, X., Müller, M., Jiang, S., Wu, Y., Zhu, X., Mujahid, A., Zhu, Z., Muhamad, M. F., Sia, E. S. A., Jang, F.  
573 H. A. and Zhang, J.: Distribution and Flux of Dissolved Iron of the Rajang and Blackwater Rivers at Sarawak,  
574 Borneo, *Biogeosciences Discuss.*, 1–31, doi:<https://doi.org/10.5194/bg-2019-204>, 2019.
- 575 Zhou, Y., Martin, P. and Müller, M.: Composition and cycling of dissolved organic matter from tropical peatlands  
576 of coastal Sarawak, Borneo, revealed by fluorescence spectroscopy and parallel factor analysis, *Biogeosciences*,  
577 16(13), 2733–2749, doi:10.5194/bg-16-2733-2019, 2019.

579

580 **Table 1.** Mean and standard deviation (mean±sd) of pH, conductivity and main elemental concentrations of the white river, and upstream of the white river, black river and  
 581 drainage canals for the two sampling campaigns (June: drier period, January, wetter period). DO: Dissolved oxygen, FI: Fluorescence Index, SUVA: Specific UV Absorbance).

		n	pH /	DO mg L <sup>-1</sup>	Cond μS cm <sup>-1</sup>	SM mg L <sup>-1</sup>	DOC mg L <sup>-1</sup>	N-NO <sub>3</sub> μmol L <sup>-1</sup>	N-NH <sub>4</sub> μmol L <sup>-1</sup>	P-PO <sub>4</sub> μmol L <sup>-1</sup>	Cl <sup>-</sup> mg.L <sup>-1</sup>	δ <sup>13</sup> DOC ‰	FI -	SUVA L.mg <sup>-1</sup> .m <sup>-1</sup>
White River	dry	5	5.2 ± 0.33	4.49 ± 0.26	37.2 ± 13.2	47.9 ± 13.2	8.43 ± 1.61	0.192 ± 0.062	<DL	<DL	4.83 ± 4.03	-29.46 ± 0.23	1.63 ± 0.08	3.4 ± 0
	wet	5	4.43 ± 0.86	3.37 ± 0.96	1220.6 ± 981.8	21.1 ± 2.5	11.25 ± 4.29	0.043 ± 0.049	<DL	0.003 ± 0.249	409 ± 342	-29.41 ± 0.41	1.64 ± 0.04	4.6 ± 0.3
White River upstream	dry	2	5.45 ± 5.71	4.91 ± 0.17	24 ± 3.8	55.7 ± 17.2	6.89 ± 1.28	0.196 ± 0.033	<DL	<DL	1.31 ± 0.64	-29.32 ± 0.06	1.54 ± 0	n.a
	wet	3	5.37 ± 0.06	4.15 ± 0.39	268.7 ± 92	29.4 ± 10.1	8.69 ± 0.78	0.061 ± 0.011	<DL	0.005 ± 0.404	47.9 ± 65.2	-29.56 ± 0.13	1.57 ± 0.01	4.1 ± 0.1
Black river	dry	8	3.45 ± 0.06	1.69 ± 0.39	98.7 ± 18.2	23.7 ± 19.1	36.42 ± 2.54	0.092 ± 0.042	0.120 ± 0.091	0.023 ± 2.32	2.78 ± 0.5	-30.29 ± 0.38	1.7 ± 0.04	4.8 ± 0.4
	wet	11	2.97 ± 0.13	1.98 ± 0.75	77.3 ± 18.3	13.4 ± 8.5	35.37 ± 3.7	0.043 ± 0.022	0.014 ± 0.028	0.014 ± 1.22	2.2 ± 0.6	-30.04 ± 0.38	1.8 ± 0.09	4.9 ± 1.3
Drainage canal	wet	6	3.08 ± 0.43	2.34 ± 0.3	89.8 ± 19.6	n.a	35.17 ± 5.47	0.034 ± 0.033	0.020 ± 0.039	0.021 ± 1.65	2.6 ± 0.6	-30.27 ± 0.4	1.8 ± 0.13	4.3 ± 1.3

582



583

584 **Table 2.** Mean and standard deviation (mean±sd) of trace meatal concentration of the white river, white river  
 585 tributaries, black river and drainage canals for the two sampling campaigns (June: drier period, January, wetter  
 586 period).

	n	Al μg.L <sup>-1</sup>	Fe μg.L <sup>-1</sup>	Ni μg.L <sup>-1</sup>	Cu μg.L <sup>-1</sup>	Zn μg.L <sup>-1</sup>	Pb μg.L <sup>-1</sup>
White River	5			0.53 ±	1.14 ±		0.262 ±
	dry	312 ± 407.1	444.9 ± 383.9	0.11	0.16	18.57 ± 9.028	0.236
	we	147.2 ±		1.19 ±	0.87 ±		0.129 ±
White River upstream	5	124.6	547.5 ± 497.3	1.17	0.09	10.26 ± 6.14	0.102
	dry	101.61 ±		0.52 ±	1.06 ±		0.139 ±
	we	27.5	242.5 ± 44.5	0.08	0.01	15.29 ± 3.06	0.027
Black river	3			0.72 ±	1.19 ±		0.236 ±
	t	148.6 ± 72	408.7 ± 170.2	0.44	0.24	9.7 ± 6.23	0.167
	8		2143.5 ±	1.96 ±	0.58 ±	119.38 ±	0.467 ±
Drainage canal	dry	592.8 ± 43	187.6	1.67	0.19	86.47	0.054
	we	443.1 ±			0.72 ±		
	t	137.5	1441 ± 493.5	1.3 ± 0.53	1.13	10.95 ± 6.98	0.316 ± 0.11
Drainage canal	we	489.2 ±			0.37 ±		0.313 ±
	t	194.9	1348 ± 494.1	1.54 ± 0.8	0.07	14.52 ± 11.62	0.048

587

588

589

590

591

592

593

594

595

596

597

598

599

600

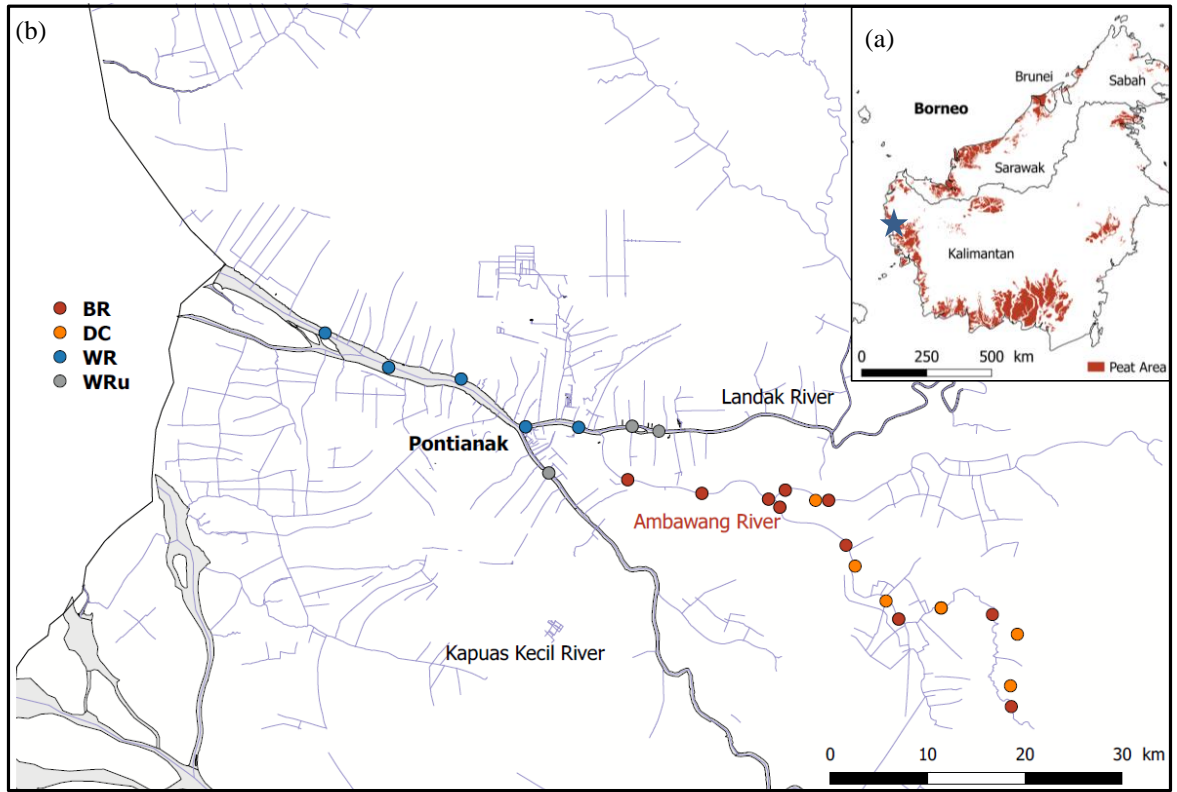
601 **Table 3.** Proportion of DOC and selected trace metals in the form of dissolved and fine colloids (< 0.22 μm) and  
 602 coarse colloids (0.2-2.7 μm)

603

	Drainage Canals		Black River		White River	
	<0.2 μm	0.2-2.7 μm	<0.2 μm	0.2-2.7 μm	<0.2 μm	0.2-2.7 μm
DOC	97	3	98	2	100	0
Al	39	61	36	64	18	82
Fe	100	0	99	1	45	55
Pb	75	25	78	22	34	66
As	98	2	96	4	67	33
Ni	72	28	50	50	1	99
Cu	68	32	48	52	1	99
Zn	13	87	12	88	26	74
Cd	66	34	100	0	83	17

604

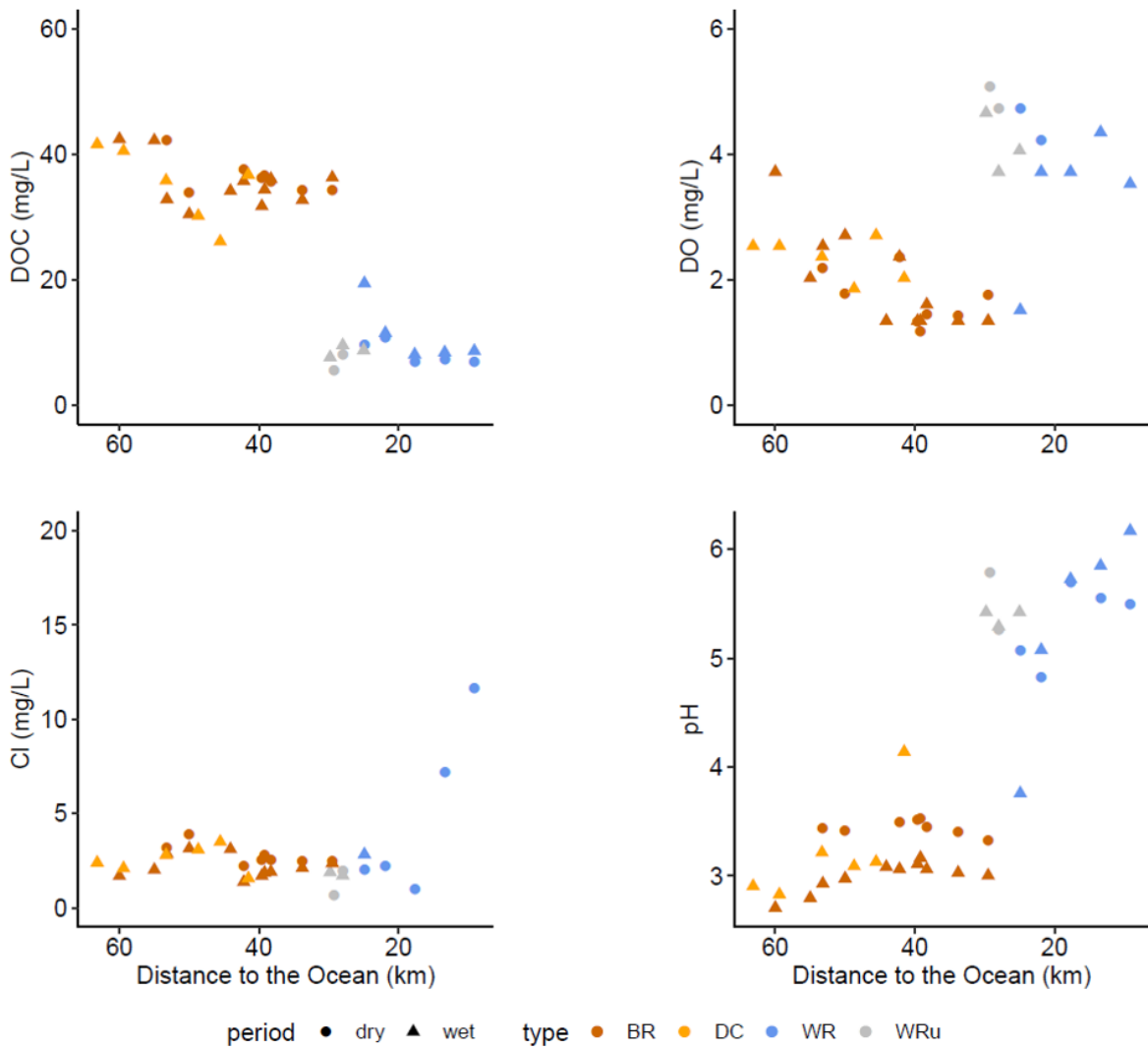
605  
606  
607  
608



609  
610  
611  
612  
613  
614  
615

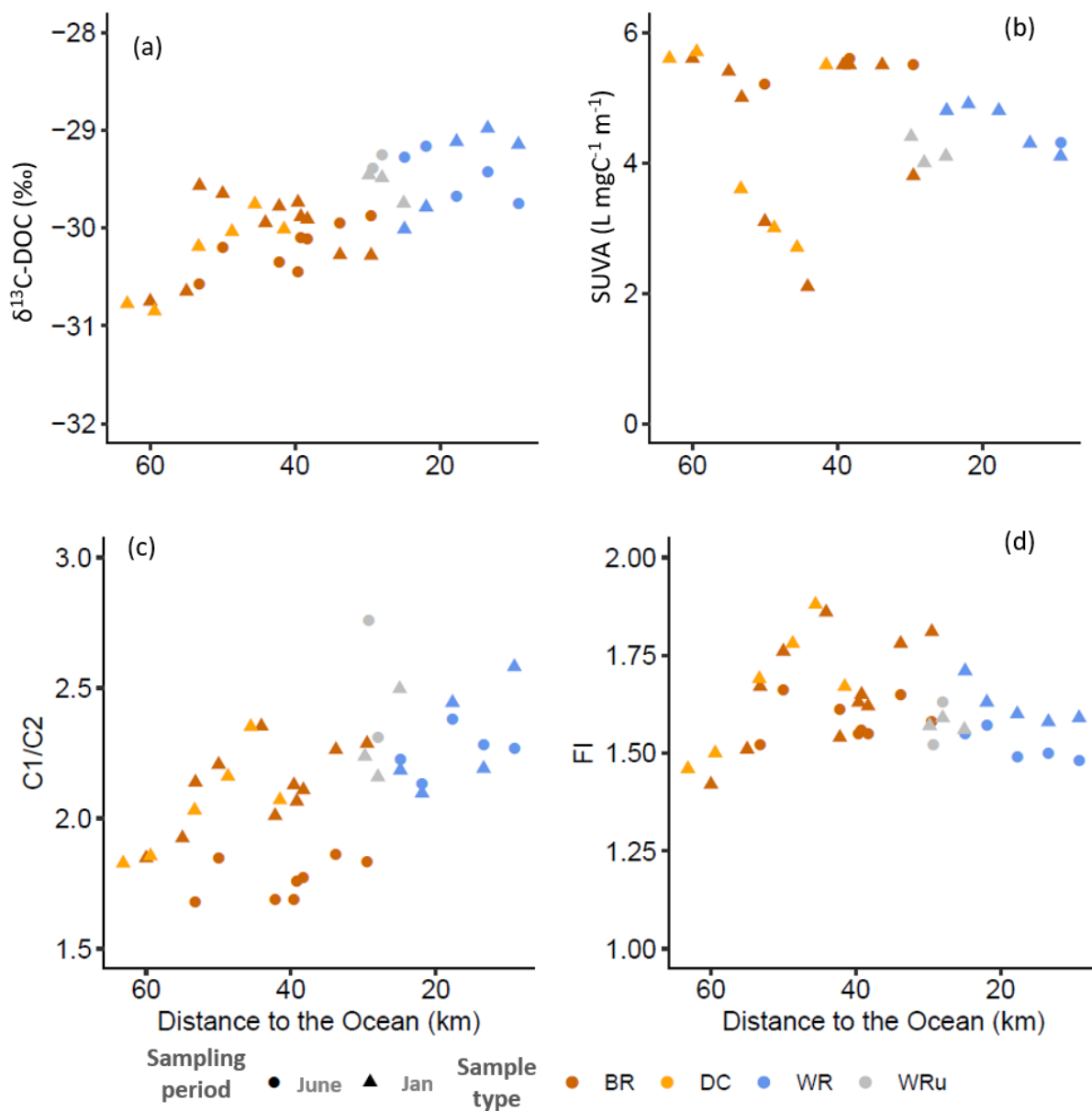
**Figure 1:** (a) Location of the study area on Borneo island. (b) Location of sampling sites and types of water: Black River (BR). Drainage Canals (DC). White River (WR). and white River upstream of the confluence with the black river (WRu).

616  
617  
618  
619  
620  
621  
622



623  
624  
625  
626  
627  
628  
629

**Figure 2:** Evolution of (a) dissolved organic carbon concentration. (b) dissolved oxygen concentration. (c) chloride concentration and (d) pH along the continuum from the black river to the ocean.



631

632

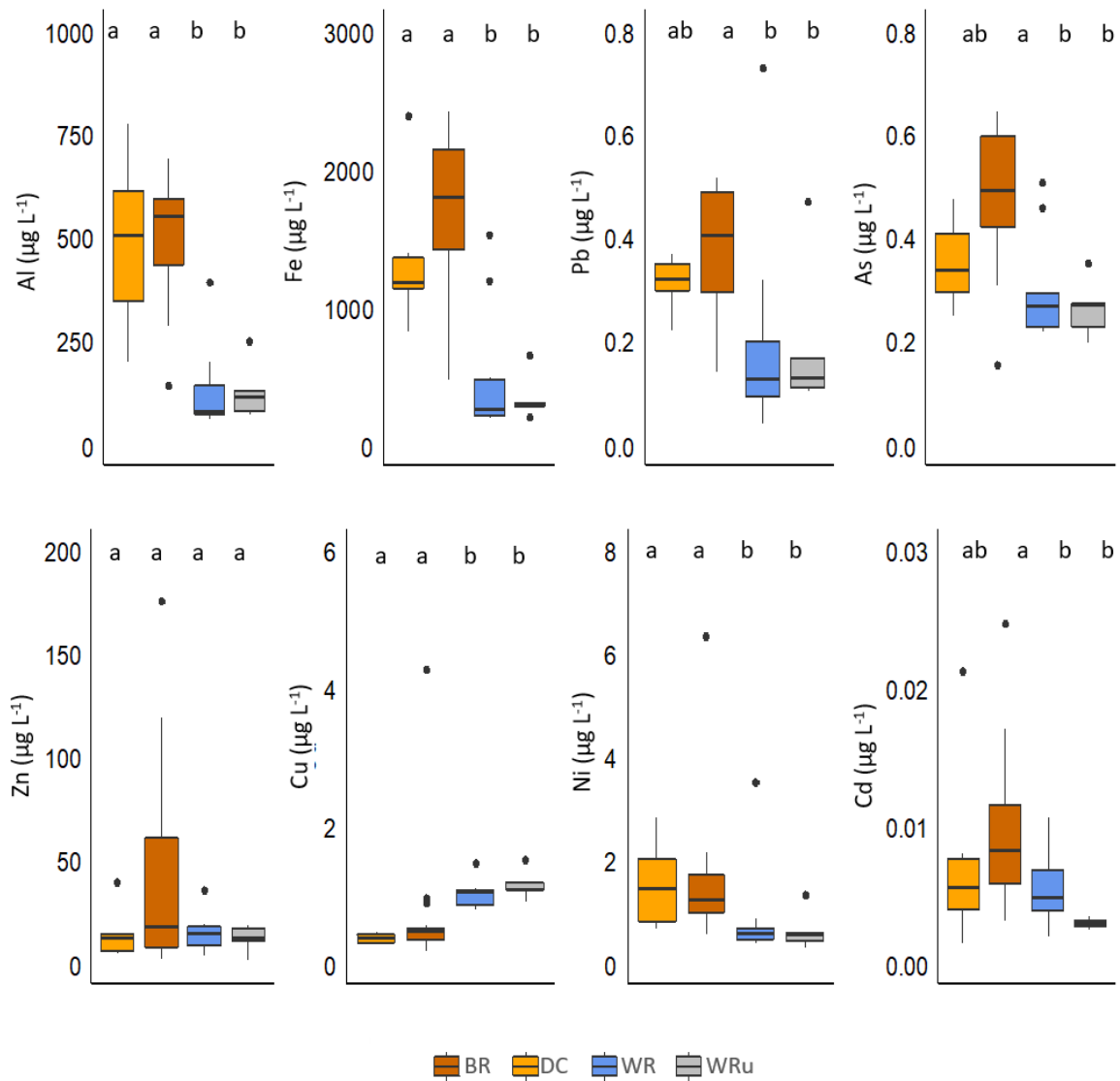
633

634

635

636 **Figure 3:** Evolution of DOM along the black river to the ocean continuum. (a)  $\delta^{13}\text{C-DOC}$ . (b) SUVA (Specific  
637 UV Absorbance) index. (c) C1/C2. (d) FI (Fluorescence Index).

638

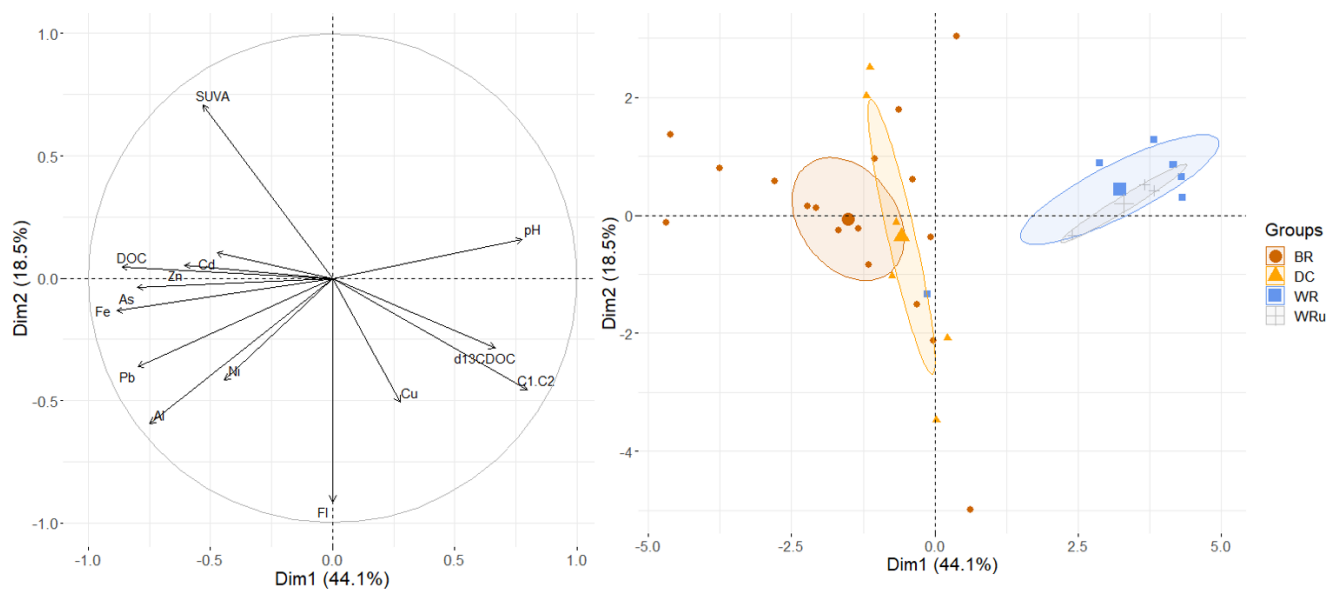


639  
 640  
 641  
 642  
 643  
 644

645 **Figure 4:** Ranges of selected TM concentration for different sampled water types. Letters represent significantly  
 646 different groups (Kruskall Wallis and Dunn's post hoc multiple test ( $p < 0.05$ )). The black line is the median. The  
 647 lower and upper levels of the box represent the 25 and 75 % quartile, respectively. The lower whisker is smallest  
 648 observation greater than or equal to lower hinge -  $1.5 * \text{IQR}$  (inter-quartile range). the upper whisker, the upper  
 649 whisker is the largest observation less than or equal to upper hinge +  $1.5 * \text{IQR}$ .

650  
 651  
 652

653  
654  
655  
656  
657  
658  
659



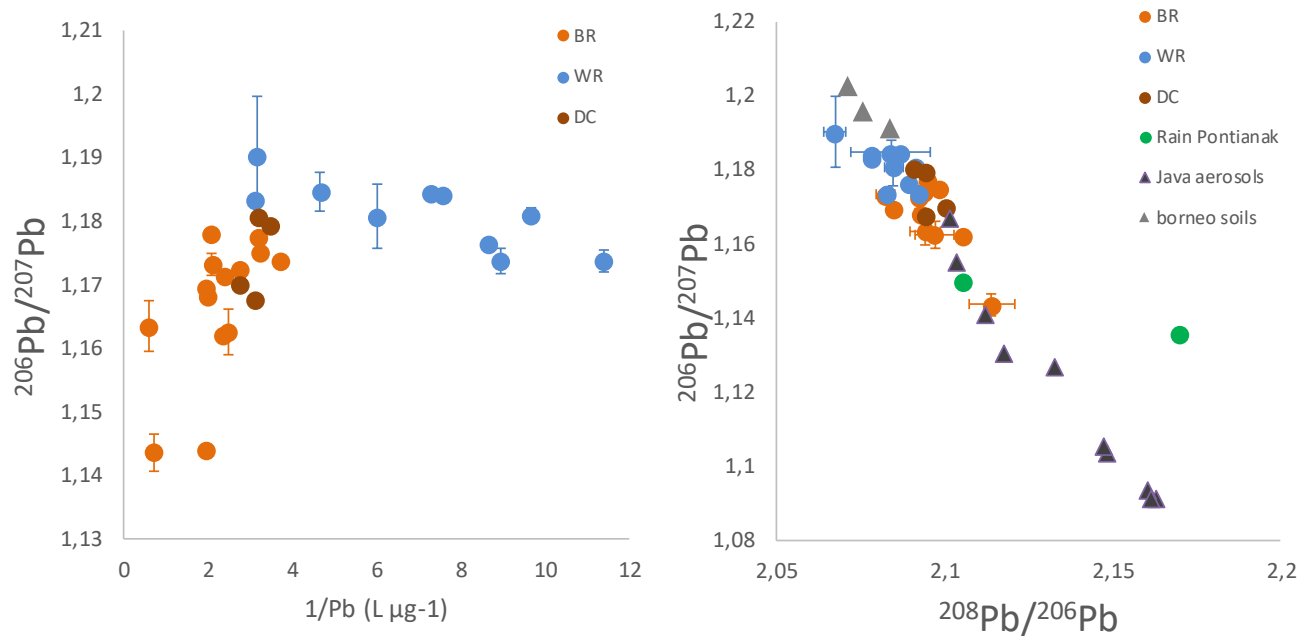
660  
661  
662  
663  
664  
665  
666  
667  
668  
669  
670  
671  
672  
673  
674

**Figure 5:** The first two factors of the PCA (63.1 % of variance) by variables (a) and by observation (b) for the different sampled water types.

675

676

677



678

679

680 **Figure 6:** (a) Dependence of  $^{206}\text{Pb}/^{207}\text{Pb}$  ratio on Pb concentrations for the different water samples. (b) Relationship  
681 between  $^{206}\text{Pb}/^{207}\text{Pb}$  ratio and  $^{208}\text{Pb}/^{206}\text{Pb}$  ratio. The error bars represent the +/- standard deviation.

682 .

683

684